

***Final Draft***  
**of the original manuscript:**

Brunke, E.-G.; Walters, C.; Mkololo, T.; Martin, L.; Labuschagne, C.;  
Silwana, B.; Slemr, F.; Weigelt, A.; Ebinghaus, R.; Somerset, V.:

**Mercury in the atmosphere and in rainwater at Cape Point,  
South Africa**

In: Atmospheric Environment (2015) Elsevier

DOI: [10.1016/j.atmosenv.2015.10.059](https://doi.org/10.1016/j.atmosenv.2015.10.059)

# Mercury measurements (2007-2013) made in the atmosphere and in rainwater at Cape Point, South Africa

Ernst-Günther Brunke<sup>1</sup>, Chavon Walters<sup>2</sup>, Thumeka Mkololo<sup>1</sup>, Lynwill Martin<sup>1</sup>, Casper Labuschagne<sup>1</sup>, Bongwiwe Silwana<sup>2</sup>, Franz Slemr<sup>3</sup>, Andreas Weigelt<sup>4</sup>, Ralf Ebinghaus<sup>4</sup>, and Vernon Somerset<sup>2‡</sup>

<sup>1</sup>South African Weather Service c/o CSIR, P.O. Box 320, Stellenbosch 7599, South Africa

<sup>2</sup>Natural Resources and the Environment (NRE), Council for Scientific and Industrial Research (CSIR), Stellenbosch, 7600, South Africa.

<sup>3</sup>Max-Planck-Institut für Chemie, Hahn-Meitner-Weg 1, 55128 Mainz, Germany

<sup>4</sup>Helmholtz-Zentrum Geesthacht (HZG), Institute of Coastal Research, Max-Planck-Strasse 1, D-21502 Geesthacht, Germany,

## Abstract

Mercury measurements were concurrently made in air (Gaseous Elemental Mercury, i.e. GEM) as well as in precipitation samples (Total mercury, i.e. TotHg) over a seven year period (2007-2013) at Cape Point, South Africa, during the rainy seasons (May – October). Eighty-five rain events, almost exclusively associated with cold fronts, have been identified of which 75% reached the Cape Point observatory directly across the Atlantic Ocean from the south, while 19% moved in to the measuring site via the Cape Town metropolitan region. In statistic terms the GEM, TotHg, CO and <sup>222</sup>Rn levels within the urban-marine events do not differ from those seen in the marine rain episodes. Over the 2007 – 2013 period, the May till Oct averages for GEM ranged from 0.913 ng m<sup>-3</sup> to 1.108 ng m<sup>-3</sup>, while TotHg concentrations ranged from 0.03 to 52.5 ng L<sup>-1</sup> (overall average: 9.91 ng L<sup>-1</sup>). A positive correlation ( $R^2 = 0.49$ ,  $n=7$ ) has been found between the average annual (May till October) GEM concentrations in air and TotHg concentration in rainwater suggesting a close relationship between the two species. The wetter years are normally associated with higher GEM and TotHg levels. Both GEM and TotHg annual means correlate positively with total annual (May till October) rain depths. If one or two outlier years are removed from the data set the  $R^2$  values for the averages from the remaining years increases to 0.97 ( $n=5$ ) and 0.89 ( $n=5$ ) for GEM and TotHg, respectively. The relationship between annual mean GEM and annual precipitation depth also holds for the period 1996-2004 ( $R^2 = 0.6$ ,  $n=8$ ) when GEM was measured manually (low resolution data). A positive correlation was also seen between annual average GEM concentrations and the El Niño Southern Oscillation (ENSO) Index (SOI), for the 1996-2004 period ( $R^2 = 0.7$ ,  $n=8$ ). For the 2007-2013 periods this relationship was also positive but less pronounced. The relationship between annual precipitation depth and annual SOI suggests that the inter-annual variations of GEM (Hg<sup>0</sup>) concentration might be caused by large-scale meteorological processes including variations in sea surface temperatures which could affect air-sea flux processes as well as changes in long-range transport and precipitation patterns.

**Keywords:** Gaseous Elemental Mercury; Atmospheric; Total mercury; Rainwater; Cape Point

## 1. Introduction

Mercury (Hg) is regarded as a highly toxic heavy metal and is also considered a global pollutant due to its long range transport and its bio-accumulation in the aquatic nutrition chain. Mercury is discharged into the atmosphere through both natural and anthropogenic sources. Atmospheric Hg consists mostly of gaseous elemental mercury (GEM), with small fractions of

---

<sup>‡</sup> Vernon Somerset; Tel.: +27.21.8882631; Fax: +27.86.6631789; Email: [vsomerset@csir.co.za](mailto:vsomerset@csir.co.za); [vsomerset@gmail.com](mailto:vsomerset@gmail.com)

51 gaseous oxidized mercury (GOM) and particle bound mercury (PBM) which together usually  
52 represent less than 3% of total atmospheric mercury (Schroeder and Munthe, 1998; Lindberg et  
53 al., 2007, Sprovieri et al., 2010). Because of its high vapour pressure and low solubility, GEM  
54 has to be oxidized to RGM to be removed from the atmosphere. In contrast to GEM, RGM and  
55 PM are readily removed from the atmosphere by rain and washout as well as by dry deposition  
56 (Lindberg et al., 2007). Wet and dry deposition thus represents an important source of mercury  
57 to terrestrial and aquatic systems (Mason and Sullivan, 1998; Prestbo and Gay, 2009) and as  
58 such is often used to assess the adverse effects of Hg (Fitzgerald et al., 1998; Kotnik et al.,  
59 2002). Long-term measurements of rainwater Hg have been reported by several authors  
60 worldwide, but most of the present monitoring sites are located in the Northern Hemisphere  
61 (NH) (Mason et al., 2000; Laurier and Mason, 2007; Dutt et al., 2009; Prestbo and Gay, 2009;  
62 Gratz et al., 2009; Caffrey et al., 2010; Lombard et al., 2011). Only a few measurement of Hg in  
63 rainwater have been reported in the Southern Hemisphere (SH) so far (Lamborg et al., 1999;  
64 Mirlean et al., 2005; Dutt et al., 2009, Gichuki and Mason, 2013).

65 In Southern Africa, limited work has been conducted to understand the factors that  
66 influence the atmospheric wet and dry deposition of Hg (Gichuki and Mason 2013;  
67 Masekoameng et al., 2010). In the study conducted by Williams et al. (2011) mercury was  
68 measured in the water management area and reported values ranged between 1.51-2.00 ng/L and  
69 20.01-50.00 ng/g for TotHg in water and sediment samples, respectively. Similarly, for Southern  
70 America and Australia, limited work has been conducted to characterise Hg in precipitation,  
71 although a few studies have reported TotHg concentrations in wet deposition and watershed  
72 studies (Mirlean et al., 2005; Biester et al., 2002; Dutt et al., 2009; Lamborg et al., 1999).

73 GEM has been measured at Cape Point, South Africa, between 1995 and 2004 and since  
74 2007 until present. Different aspects of these measurements have been reported in the literature  
75 such as the GEM seasonality (Slemr et al., 2008), long-term trends (Slemr et al., 2011),  
76 occasional depletion events (Brunke et al., 2010), and the use of the data for the estimation of  
77 anthropogenic emissions and terrestrial fluxes in southern Africa (Brunke et al., 2012; Slemr et  
78 al., 2013). Measurements of TotHg in rainwater have been made since June 2007 and the first  
79 results for the period from 2007 until December 2009 were already reported by Gichuki and  
80 Mason (2013). They presented a seasonal analysis of TotHg concentrations in wet deposition  
81 samples. The results of their study have also shown that both marine and continental air masses  
82 classified via  $^{222}\text{Rn}$  and CO (Brunke et al., 2012) could influence the measured TotHg  
83 concentrations in wet deposition at Cape Point. They emphasized the need for more accurate  
84 long-term TotHg measurements in order to improve our understanding of the chemical and  
85 atmospheric processes driving deposition at Cape Point and its links between GEM measured at  
86 the same site.

87 The data presented in this study provides a summary of Cape Point GEM and TotHg  
88 concentrations measured until the end of 2013, their inter-annual variations, their relationship  
89 among themselves and with meteorological parameters such as annual precipitation depth and El  
90 Niño Southern Oscillation (ENSO). The findings from the analysis of this extended data set  
91 reveal new insights into the relation between GEM, TotHg, and meteorological parameters.

92  
93

## 94 **2. Study Site and Methods**

95

### 96 2.1. Geographic Location and Climate

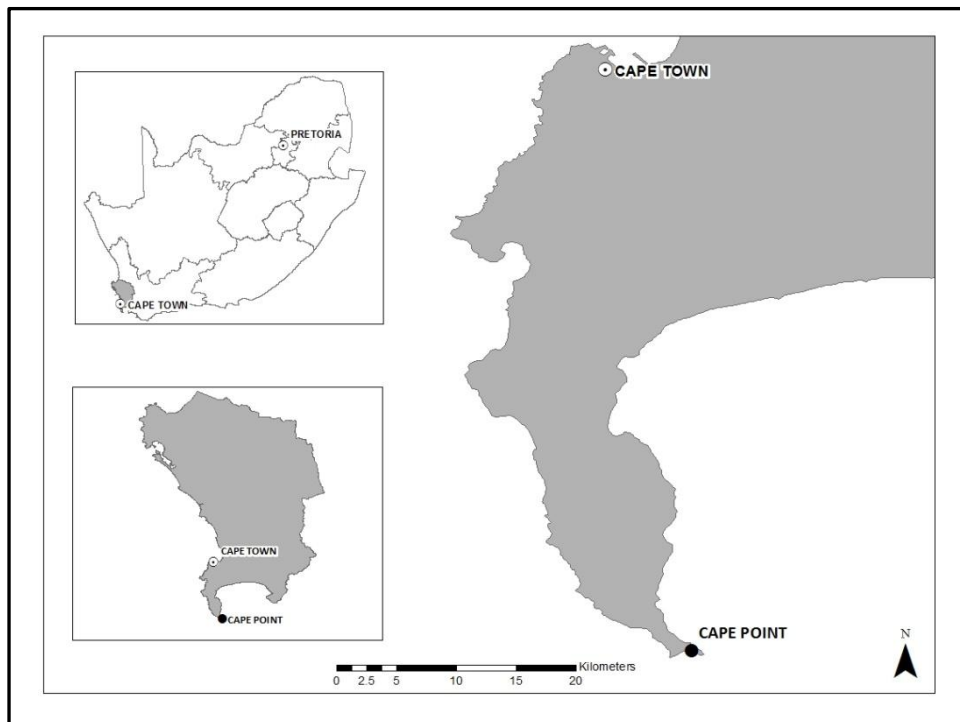
97

98 The Cape Point Global Atmosphere Watch (GAW) station (34° 21'S, 18° 29'E) is managed by  
99 the South African Weather Service (SAWS) and is one of more than 30 GAW baseline stations  
100 of the World Meteorological Organisation (WMO). The laboratory is located about 60 km to the

101 south of the greater Cape Town area (Fig. 1). It is situated within a National Park at the southern  
102 tip of the Cape Peninsula on top of a cliff (230 m a.s.l.). The station has been in operation since  
103 1978 and its current continuous measuring program includes Hg (GEM), CO, <sup>222</sup>Rn, surface O<sub>3</sub>,  
104 CH<sub>4</sub>, N<sub>2</sub>O, CO<sub>2</sub>, halocarbon species (e.g. CFC-11 and 12), aerosol optical density and optical  
105 properties, as well as solar and meteorological parameters (<http://gaw.empa.ch/gawsis>).

106 Cape Point experiences a Mediterranean-type climate that is characterized by rather dry  
107 summers comprising moderate temperatures. The austral autumn to spring season (May till  
108 October) normally experience increased precipitation due to the passage of cold fronts moving  
109 from West to East. Furthermore, the prevailing wind direction at Cape Point during austral  
110 summer is mainly from the southeast to the southwest, while during winter the air is more  
111 strongly advected to the station from the north to northwestern quadrant (Rautenbach and Smith  
112 2001; Brunke et al., 2004). As such Cape Point generally receives clean marine air from the  
113 Southern Atlantic, especially during the summer months. However, at times (mainly during the  
114 winter period) continental and polluted air masses are observed at the site more frequently. The  
115 polluted events provide interesting data, but can easily be filtered out using <sup>222</sup>Rn as an effective  
116 tracer for maritime air (Brunke et al., 2004). This procedure is applied routinely for the purposes  
117 of detecting long-term trends for trace gases, such as CO<sub>2</sub>, CH<sub>4</sub>, CO and others under  
118 background conditions.

119  
120



121  
122

123 Fig. 1: Map showing the location of Cape Town, Pretoria and Cape Point at the southern end of  
124 the Cape Peninsula with Cape Town 60 km to the north.

125  
126

127 The main source of Hg in the South African environment is from anthropogenic  
128 emissions mostly due to burning low grade coal at coal-fired power stations, the main source of  
129 energy production in South Africa (Dabrowski et al., 2008; Masekoameng et al., 2010; Williams  
130 et al., 2010). Other anthropogenic sources that may also play a role are from waste incineration,  
131 biomass burning, cement production and artisanal gold mining (Gichuki and Mason, 2013;  
132 Dabrowski et al., 2008). Although the greater Cape Town area emits mercury (e.g. from diesel

133 driven vehicles and waste incineration), the major anthropogenic Hg sources are located 1500 –  
134 2000 km to the north-west of Cape Point in the Gauteng and Mpumalanga provinces where  
135 former mine dumps from gold mining (Dabrowski et al., 2008) and large coal-burning power  
136 stations are located. Although Cape Point is subjected mainly to the advection of marine air,  
137 continental air also reaches the station, especially during the winter months thereby bringing  
138 with it traces of local and regional pollution (Brunke et al., 2004). However, the major source  
139 region affecting Cape Point GEM levels is thought to be located in the Southern Ocean as is  
140 indicated by back trajectory studies (Brunke et al., 2004).

141

## 142 2.2. Measurements and Analysis

143

### 144 2.2.1. Atmospheric mercury sampling

145 GEM has been measured at Cape Point by a manual amalgamation technique (Slemr et  
146 al., 2008) since September 1995 until December 2004 and by a Tekran 2537A instrument  
147 (Tekran Inc., Toronto, Canada; Steffen and Schroeder, 1999) since March 2007. The manual  
148 technique provided about 200 GEM concentrations per year, each averaged over a 3 h sampling  
149 time. In this paper we use primarily the latter data with a resolution of 15 min. The start of the  
150 highly resolved GEM measurements in 2007 roughly coincides with the commencement of the  
151 CSIR's Hg precipitation project (Gichuki and Mason, 2013). The air measurements were made  
152 in compliance with the standard operating procedures of the GMOS (Global Mercury  
153 Observation System, www.gmos.eu) project.

154

### 155 3.2.2. Rainfall collection and analysis

156 Weekly precipitation samples were collected as a continuation of the project started by  
157 Gichuki and Mason (2013) in June 2007 almost exclusively during the rainy season which at  
158 Cape Point lasts from May till October. The sample equipment cleaning protocol and sample  
159 collection generally consisted of standard protocols for TotHg in acid-cleaned Teflon® bottles  
160 (US EPA, 1996; Williams et al., 2011). Rainwater samples were collected using a homemade  
161 glass funnel connected to a 500 mL Teflon® bottle (Gichuki and Mason, 2013). After each  
162 weekly sample the Teflon® sampling bottle was disconnected from the rain funnel and the  
163 sample was preserved by spiking it with 0.5% (v/v) trace metal grade hydrochloric acid solution,  
164 followed by sample refrigeration during storage.

165 The analytical protocol for the rain sample comprised the digestion with bromine  
166 chloride (BrCl) and reduction with hydroxylamine hydrochloride (NH<sub>2</sub>OH.HCl) and stannous  
167 chloride (SnCl<sub>2</sub>.2H<sub>2</sub>O). The released elemental Hg vapour was trapped by amalgamation on a  
168 gold surface and was detected after thermo-desorption by cold vapour atomic fluorescence  
169 spectrometry (CVAFS). Rainwater volumes were recorded for each sampling events. Data are  
170 presented as volume-weighted mean (VWM) Hg concentrations (ng/L) for each weekly sample  
171 (Williams et al., 2011; Gichuki and Mason, 2013).

172

### 173 3.2.3. Atmospheric gases and precipitation data organisation

174 The sampler was exposed for one week at a time, i.e. from one Monday till the next and  
175 thus collected some mercury by dry deposition, which - according to Gichuki and Mason (2013)  
176 - is negligible. Over the seven year period, 138 weekly samples were collected, of which 12  
177 samples were dry (no rain water at all) leaving a total of 126 wet samples. Of these weekly  
178 samples a few constituted more than one event, while a few others were too small to be  
179 analysed.

180 In our approach to identify meaningful rainfall events (ranging from hours to a few days)  
181 we used 30 min average rainfall data obtained from the SAWS automatic rain gauge. If rain was  
182 collected continuously over a period of three hours or more and exceeded a total rain depth of 6  
183 mm, it was classified as a rain event. A precipitation gap exceeding five hours or more was  
184 arbitrarily chosen to separate different rain events from one another. The half-hourly  
185 precipitation maximum of an event was selected to represent the temporal apex for that episode.  
186 In accordance, the respective GEM, CO and  $^{222}\text{Rn}$  median - in addition to the total rain depth  
187 (total volume water collected) - were determined for the duration of each respective event and  
188 assigned to the time stamp of that rain maximum. In total, 85 rain events out of the 126 wet  
189 weekly samples have been identified to meet these criteria. Notwithstanding, the somewhat  
190 subjective approach in identifying the start and end times of each rainfall episode, we are  
191 confident that this method is more accurate than simply working with the composite weekly  
192 samples and assigning supplementary data to them.

193 Whilst low  $^{222}\text{Rn}$  concentration is an excellent tracer for marine air (Brunke et al., 2004),  
194 elevated CO levels represent a good indicator of anthropogenic activities (Scheel et al., 1998).  
195 Since CO has a strong annual cycle (Seiler et al., 1984), the data have been de-seasonalised so  
196 that CO concentrations investigated here can be related to any marine and urban-continental  
197 signatures unaffected by CO's seasonality. An arbitrary offset was applied to the de-seasonalised  
198 CO time series so that minimum levels approximated 27 ppb. All values exceeding 27 ppb are  
199 hence due to urban-continental signatures.

200  
201

### 202 **3. Results and Discussion**

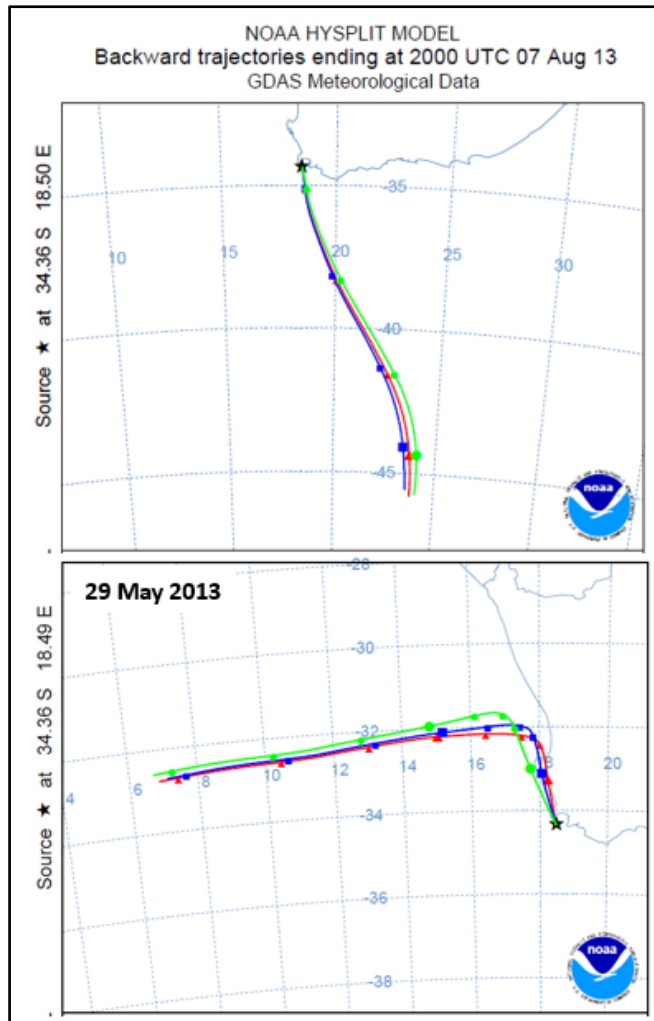
#### 203 3.1. Backward trajectories for rain events

204  
205 Ten-day isentropic back trajectories (NOAA Hysplit Model; <http://www.arl.noaa.gov/HYSPLIT.php>.) with 4-hourly resolution and a 500m arrival altitude were generated for the 85  
206 rain events identified during 2007 - 2013. The time of the highest rain intensity (apex) observed at  
207 the station during a rain episode was selected as the arrival time of the respective air mass  
208 trajectory for that event.

209  
210 It was found that almost all cold fronts which led to rain events were associated with  
211 trajectories originating from the Atlantic Ocean. There were no rain events of continental origin.  
212 Of the rain events identified, 75% correspond to air masses which reached Cape Point directly  
213 from within the southern quadrant ( $140^\circ$  to  $280^\circ$ ) without moving over land first. About 19% of all  
214 trajectories made a small bypass over the Cape Town metropolitan area before reaching the GAW  
215 station. The 7<sup>th</sup> of August 2013 represents an example of the former, while the 29<sup>th</sup> of May 2013 is  
216 an example of the latter trajectory type (Fig. 2). The remaining trajectories (6%) made diversions  
217 over the southern tip of Africa (Agulhas) before reaching Cape Point (not shown here), thereby  
218 possibly entraining some continental air.

219



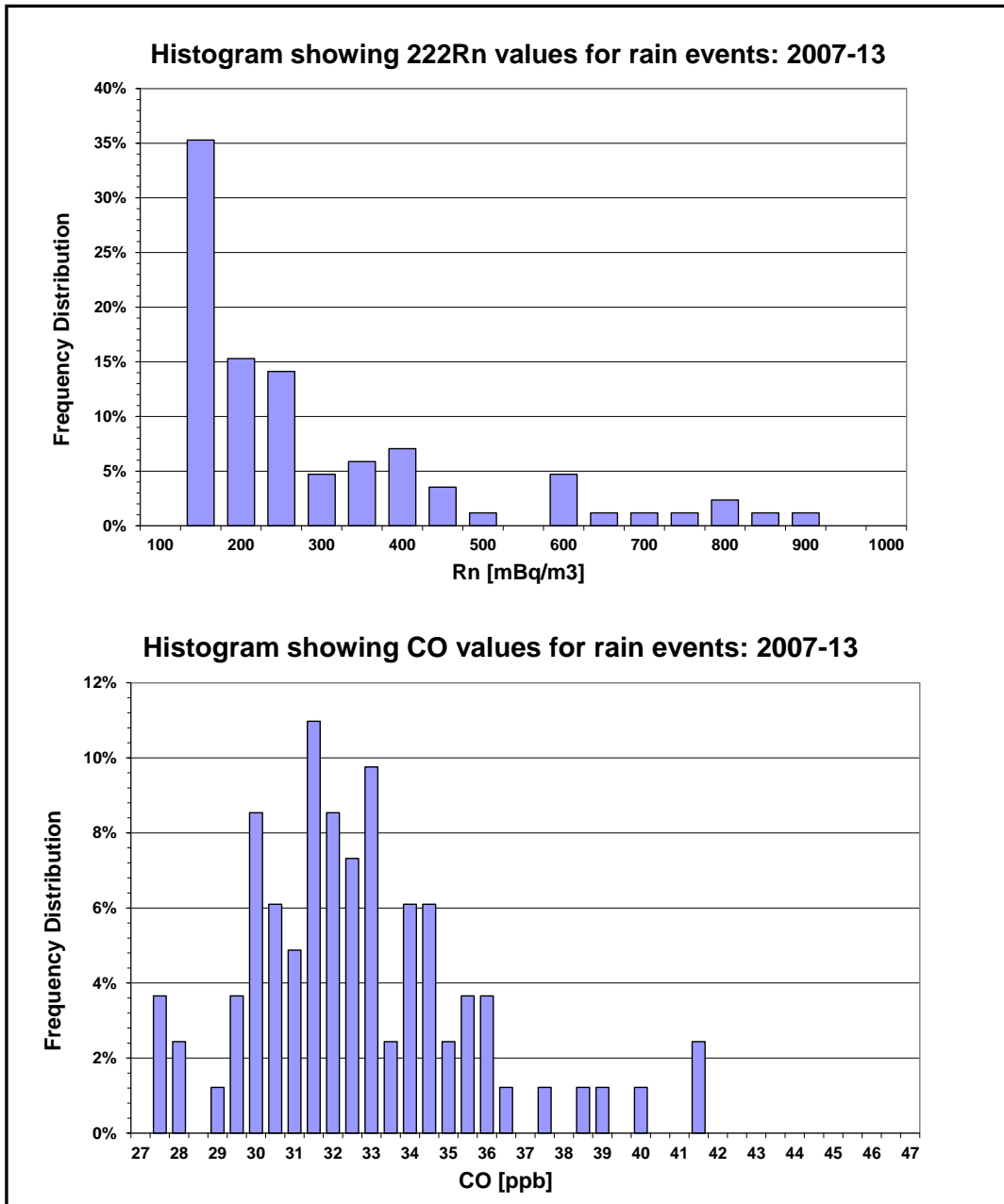


220  
221  
222  
223  
224  
225  
226

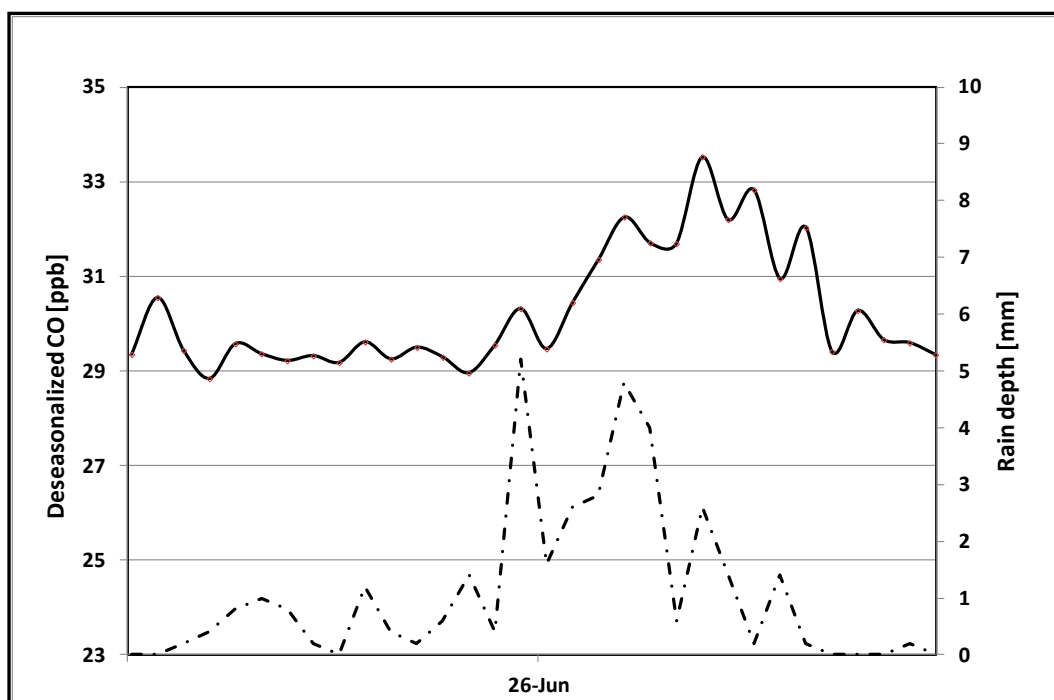
Fig. 2. Backward trajectories associated with cold fronts reaching Cape Point directly from the Southern Ocean (top) or transgressing over Cape Town first (bottom).

### 227 3.2. Air quality associated with rain events

228  
229 <sup>222</sup>Rn concentrations and de-seasonalised CO data measured during these rain events have  
230 been summarized in the histograms shown in Fig. 3. Approximately 64% of the <sup>222</sup>Rn  
231 concentrations fall below 250 mBq m<sup>-3</sup>, which is considered to represent essentially marine air  
232 (Brunke et al., 2004). Likewise, 85% of the de-seasonalised CO data fall within the range between  
233 27 to 37 ppb. The small variability of only 10 ppb shows that the influence of urban-continental  
234 air was small. As substantiated by the trajectories, we conclude that rain events are generally  
235 associated with clean marine air masses. Even if a cold front sweeps over Cape Town first, the  
236 altitude of the clouds and their limited temporal exposure to anthropogenic sources essentially  
237 precludes the uptake of pollutants in most cases.  
238







247  
248  
249  
250  
251  
252

Fig. 4. De-seasonalised CO (solid line) and rain depth (dotted line) for 25<sup>th</sup> and 26<sup>th</sup> of June 2007 revealing minimal anthropogenic influences.

253  
254  
255  
256  
257  
258  
259  
260  
261

On the 25<sup>th</sup> and 26<sup>th</sup> of June 2007 the rain event (Fig. 4) was accompanied by relatively low CO levels, which varied from 29 to 34 ppb (2 to 7 ppb above the 27 ppb CO offset) indicating only a negligible contribution from urban sources. A few instances have been observed where CO mixing ratios reached levels in the vicinity of 400 ppb (e.g. on August 1, 2009, or June, 30, 2010). However, these constitute exceptions rather than the rule and might also have been affected by the difficulty in clearly defining the temporal extent of the rain event in question, as mentioned above. In most cases the CO mole fractions varied only slightly during rain episodes – as was seen for 1<sup>st</sup> July 2010 or 22<sup>nd</sup> September 2012 – when the CO variability was within 1 ppb.

262  
263  
264  
265

Table 1: Summary statistics for GEM, TotHg, CO and <sup>222</sup>Rn (2007-2013) for marine and urban rain events. Marine rain events are defined by back trajectories directly from the southern Atlantic Ocean whereas the urban events encompass the back trajectories which crossed the greater Cape Town area.

266

267

	47 marine rain events		20 urban rain events	
Species	Average	Std dev	Average	Std dev
GEM [ng m <sup>-3</sup> ]	1.018	0.040	1.003	0.053
TotHg [ng L <sup>-1</sup> ]	8.6	8.1	10.3	11.6
CO [ppb]	32.1	1.6	35.8	5.4
<sup>222</sup> Rn [mBq m <sup>-3</sup> ]	201	74	287	188

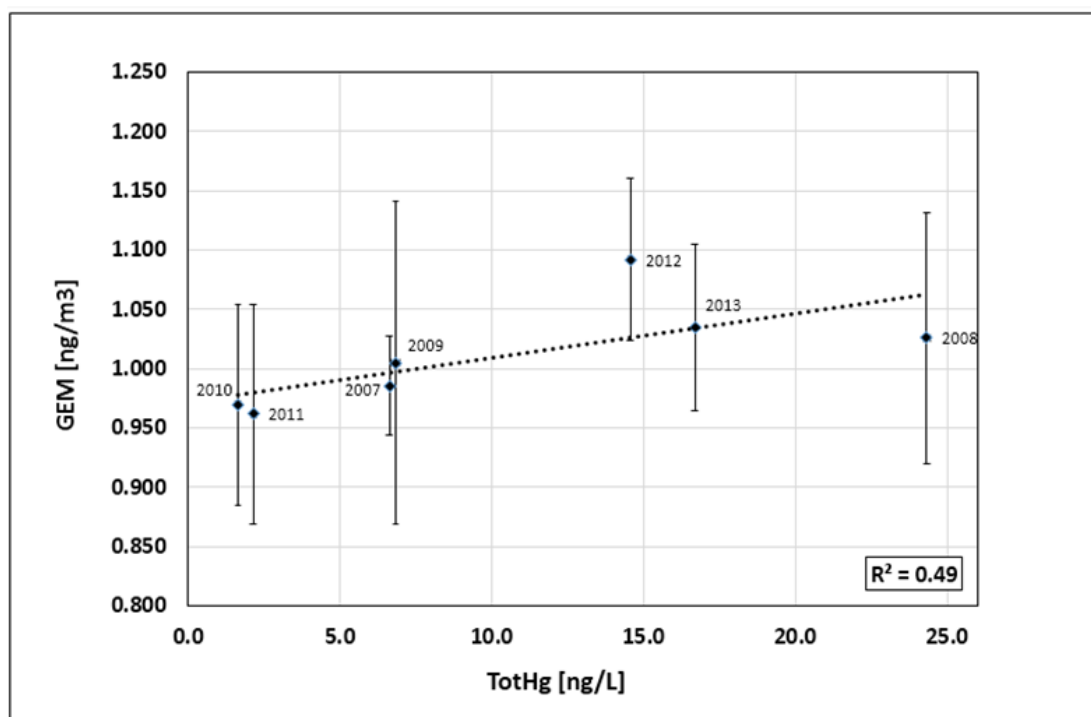
272  
273  
274  
275

Table 1 shows a summary of GEM, TotHg, CO, and <sup>222</sup>Rn concentrations measured during the rain events with back trajectories from the southern Atlantic Ocean (marine) and with back

276 trajectories which crossed the urban region of Cape Town (urban). From the 85 events 47  
 277 trajectories were typical marine and 20 typical urban. Events associated with trajectories of a  
 278 mixed nature were rejected in order to obtain a clear distinction between the two types.  
 279 Despite the significantly larger concentrations of CO (significant at > 99.9% level) and <sup>222</sup>Rn  
 280 (significant at > 99% level) during the urban type rain events, there is neither a noteworthy  
 281 difference in GEM nor in TotHg concentrations. In the case of TotHg its large standard deviation  
 282 may prevent the detection of any possible difference. However, since no difference was found in  
 283 the much less variable GEM concentrations, we conclude that the short transport of urban air  
 284 masses over the Cape Town area neither influences GEM or TotHg concentrations. Consequently,  
 285 we do not differentiate between marine and urban rain events in the following analysis.  
 286  
 287

### 288 3.3. Relationship between GEM and TotHg

289  
 290 In Figure 5 we compare GEM concentration in air with Hg found in rain samples (TotHg) during  
 291 the rainy season: averages for May till October for each year. The TotHg values in Figure 5 have  
 292 been converted to annual Volume Weighted Means (VWM) as described by [Prestbo and Gay](#)  
 293 [\(2009\)](#). Figure 5, shows a positive correlation ( $R^2 = 0.49$ ;  $n=7$ ) between annual mean GEM  
 294 concentrations and TotHg concentrations over the seven year period despite large inter-annual  
 295 variations for both. The years, 2010 and 2011 were characterized by relatively low GEM values  
 296 ( $0.970$  and  $0.962$   $\text{ng m}^{-3}$  respectively) as well as correspondingly low TotHg (VWM) levels ( $1.6$   
 297 and  $2.1$   $\text{ng L}^{-1}$  respectively). In contrast, the years 2008 and 2012 both showed rather higher Hg  
 298 values for both GEM and TotHg. For GEM:  $1.026$  and  $1.092$   $\text{ng m}^{-3}$  and for TotHg:  $24.3$  and  
 299  $14.6$   $\text{ng L}^{-1}$ , respectively.  
 300  
 301

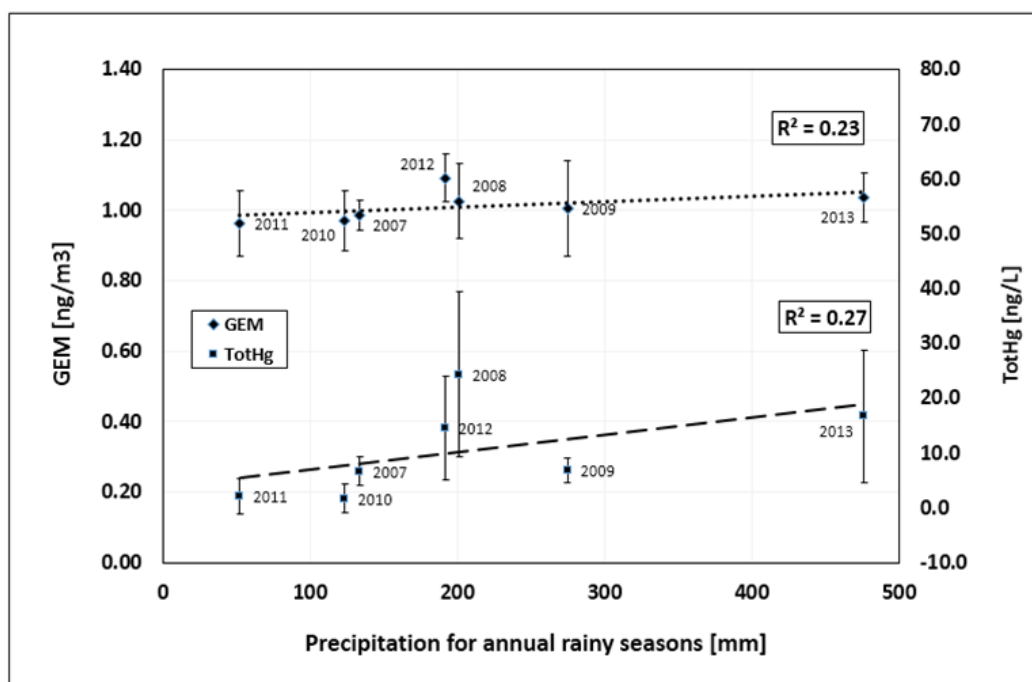


302  
 303  
 304

305 Fig. 5. Correlation plot of annual average GEM concentrations [ $\text{ng m}^{-3}$ ] vs. annual average  
 306 TotHg (VWM) [ $\text{ng L}^{-1}$ ] over the seven year period (2007-2013). Error bars represent standard  
 307 deviations and linear regression:  $\text{GEM} = 0.0037 \cdot \text{TotHg} + 0.972$ .

308  
 309  
 310 Positive correlations between total gaseous mercury (TGM) in air measured at Canadian  
 311 Atmospheric Mercury Measurement Network (CAMNet) sites and TotHg in precipitation at  
 312 nearby US Mercury Deposition Network (MDN) sites have been reported by Cole et al. (2014).  
 313 Since GOM and PBM together represented mostly about 1% of TGM (Cole et al., 2014), the  
 314 correlation also applies to GEM vs. TotHg. Both TGM and TotHg concentrations decreased with  
 315 a comparable rate between 1998 and 2011, despite steady or increasing global mercury  
 316 emissions (Wilson et al., 2010; Streets et al., 2011). This discrepancy was resolved by Soerensen  
 317 et al. (2012) who attributed the decreasing trend to declining mercury emissions from the North  
 318 Atlantic due to the reduction of mercury levels in surface sea water. The positive correlation of  
 319 TotHg vs. GEM is thus an indication that both are a function of mercury emissions. The  
 320 application of this conclusion to the Cape Point measurements raises the question as to the origin  
 321 of the inter-annual variations observed for GEM and TotHg?

322 Figure 6 shows a positive correlation of both annual average GEM concentrations and  
 323 annual average TotHg with annual precipitation (volume of collected rain sample). As can be  
 324 seen, the May – October periods for 2007, 2010 and 2011 constitute drier years, with the annual  
 325 precipitation ranging between 52 and 134 mm, while 2009 and 2013 comprise wetter years with  
 326 annual precipitation of 275 and 476 mm, respectively. The years, 2008, 2012 and 2013 are  
 327 characterised by higher standard deviations than the other years. Although the correlation factors  
 328 ( $R^2$ ) for all years are relatively small, comprising 0.23 and 0.27 for GEM and TotHg  
 329 respectively, much higher  $R^2$  values (0.97 for GEM ( $n=5$ ) and 0.89 for TotHg ( $n=5$ )) are  
 330 obtained (graph not shown here), if the extreme two years (2008 and 2012) are removed from  
 331 the data set. The relative differences between GEM and TotHg are variable (Fig. 6) and cannot  
 332 be ascribed to any identifiable process yet. Although the drier years such as 2010 and 2011 are  
 333 characterized by larger differences and the wetter years e.g. 2013 by smaller differences, this  
 334 pattern is not consistent. The years 2008 and 2012, for instance, were characterized by rather  
 335 smaller differences between GEM and TotHg and were not very wet either (197 mm rain depth).  
 336



338  
339 Fig. 6. Comparison of GEM concentrations [ $\text{ng m}^{-3}$ ] (dotted line) and TotHg [ $\text{ng L}^{-1}$ ] (dashed  
340 line) vs. annual rain depth [mm] over seven years (2007-2013). Error bars represent standard  
341 deviations. Linear regressions:  $\text{GEM} = 0.0002 * \text{Rain depth} + 0.978$  and  $\text{TotHg} = 0.0316 * \text{Rain}$   
342  $\text{depth} + 3.831$ .

343  
344  
345 The positive relationship between annual average GEM concentrations (May till  
346 October) and the corresponding annual precipitation at Cape Point was also found for the manual  
347 measurements made during 1996 - 2004 (Slemr et al., 2008). TotHg was not measured during  
348 this period. GEM average concentrations over the rainy season (May - October) vs. annual  
349 precipitation over this period shows a positive correlation ( $R^2 = 0.2$ ;  $n=8$ ). As for the high  
350 resolution data, if one or two outliers (in this case only 1998) are removed from the data set, the  
351  $R^2$  value increases to 0.6 ( $n=7$ ; with significance  $> 95\%$  confidence level; graph not shown here).  
352 The positive correlation of both GEM data sets (1996 – 2004 and 2007 - 2013) with annual  
353 precipitation lead us to suggest that the inter-annual GEM and TotHg variations in the southern  
354 hemisphere might be controlled by large-scale meteorological processes.

355  
356 3.4. Influence of El Niño Southern Oscillation (ENSO)

357  
358 Annual rainfall in Namibia and South Africa is dependent on ENSO cycles with El Niño years  
359 being drier and La Niña years being wetter (Preston-White and Tyson, 1988; Rautenbach and  
360 Smith, 2001). Consequently, good correlations between GEM and annual precipitation for the  
361 years 1996-2004 (low resolution GEM data) and 2007-2013 (high resolution GEM data) as well  
362 as between annual average TotHg concentrations and annual precipitation during the 2007-2013  
363 period suggest that both GEM and TotHg also fall under the influence of the ENSO cycles. To  
364 investigate this dependence we use the Southern Oscillation Index (SOI; <http://www.bom.gov.au/climate/current/soi2.shtml>), which is based on the observed sea level  
365 pressure difference between Tahiti and Darwin, Australia. Annual average GEM concentrations  
366 correlate positively with SOI both in the 1996-2004 (shown in Fig. 7) as well as for the 2007-  
367 2013 periods (not shown). Fig. 7 shows a positive correlation ( $R^2 = 0.7$ ;  $n=8$ , significant at  $>$   
368  $99\%$  confidence level) between GEM and the SOI for the low resolution data (1996-2004). The  
369 annual average GEM concentration for 1997 was not considered because data from May until  
370 October are missing. For the high resolution data (2007-2013), the  $R^2$  value amounts to 0.4 ( $n=6$ ,  
371 2007 removed as outlier) and is significant at  $> 90\%$  confidence level.

372  
373 TotHg (2007-2013) and rainfall (both 1996-2004 and 2007-2013 periods) were also  
374 searched for correlations with SOI. This was again done for the rainy season: May till October.  
375 However, no significant correlations have been found.

376 However, the positive relationship between GEM and the SOI is compelling (Fig. 7). It  
377 suggests either a direct influence of meteorology on GEM concentrations or an indirect one  
378 through meteorological influences on mercury emissions. A direct influence might be through  
379 sea surface temperatures which naturally have a bearing on rainfall, especially in southern Africa  
380 (Preston-White and Tyson, 1988), and/or long-range transport processes (Pirrone and Mason,  
381 2009) – also from the NH - might be controlling inter-annual variations of atmospheric Hg levels  
382 in SH mid-latitudes. Variable wind strengths could possibly also affect the Hg ocean to  
383 atmosphere flux rates (Xu et al., 2012).

384  
385

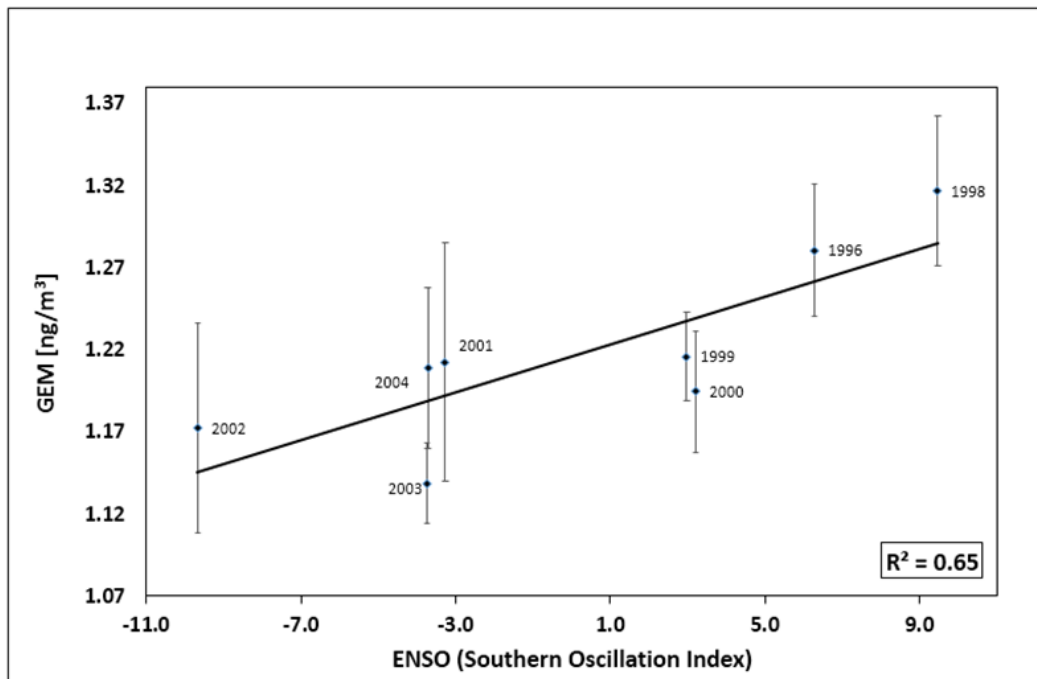


Fig. 7. Relationship between GEM averages (May till Oct) and Southern Oscillation Index (SOI, <http://www.bom.gov.au/climate/current/soi2.shtml>): 1996-2004. The error bars represent GEM standard deviations. Linear regression:  $GEM = 0.007 * SOI + 1.216$ .

The correlations between GEM and TotHg observed here and in Canada and the northeastern US suggest that both are linked to hemispheric emissions (Slemr et al., 2011; Cole et al., 2014) in the first place. Meteorological processes can influence the mercury emissions directly, e.g. by periodical changes of surface ocean temperatures during ENSO events, or indirectly via extended droughts leading to increased biomass burning. We note that oceanic emissions may represent 45% of all mercury emissions and emissions from biomass burning with a contribution of ~4% are not negligible either (Holmes et al., 2010). Meteorological processes can also influence the oxidation of GEM to species prone to rain and washout. Gratz et al. (2009) pointed out that the uptake of Hg by rainwater is a function of the effective conversion of GEM to GOM which comprises fine particle bound mercury (PBM) as well as divalent reactive gaseous mercury (RGM). However, changing oxidation rates would influence TotHg concentrations to a substantially larger degree than those of GEM and would, at constant emissions, lead to an anti-correlation between GEM and TotHg concentrations. We thus conclude that the meteorological influence on emissions is the major reason for the positive GEM vs. TotHg and GEM vs. SOI correlations.

#### 4. Conclusions

The rain episodes at Cape Point (2007-2013) are almost exclusively linked to cold fronts from the Atlantic Ocean. 75% of all air mass trajectories coupled to these rain events reach the Cape Point GAW station directly from the southern ocean, while 19% arrive there with a short bypass over the Cape Town metropolitan area. Merely 6% approach Cape Point along the sea from the East via the Cape Agulhas sub-continental region. The atmospheric levels of CO and <sup>222</sup>Rn in the identified 85 rain events are largely characteristic of maritime conditions. Although rain fronts which passed over the Cape Town region before arriving at Cape Point sometimes

419 have slightly elevated CO and  $^{222}\text{Rn}$  levels, no significant local anthropogenic influences were  
420 detected in GEM and TotHg concentrations observed at Cape Point.

421 The average GEM levels for the wet season (May till October) over the 2007-2013  
422 period show a positive correlation ( $R^2 = 0.49$ ;  $n=7$ ) with TotHg. Furthermore, the time series  
423 (2007-2013) for both GEM and TotHg in the rain events (plotted as a function of rain depth)  
424 displays similar, relative inter-annual concentration variations over the measuring period. This  
425 confirms the close coupling which exists for Hg within these two different media. If the years  
426 2008 and 2012 (rain depth about 200 mm) are removed from the data series, the  $R^2$  values  
427 improve significantly, i.e. to 0.97 for GEM and 0.89 for TotHg (VWM), respectively. Other  
428 processes might - indeed - have affected these two years which were negligible or absent in the  
429 other five years. A significant correlation has also been found between GEM and SOI during the  
430 1996-2004 period.

431 These correlations suggest that the inter-annual variations of GEM and TotHg  
432 concentrations are primarily influenced by large scale meteorology. Meteorological influences  
433 on mercury sinks e.g. through an increased oxidation rate or enhanced precipitation would, at  
434 constant emissions, lead to an anti-correlation between GEM and TotHg. The observed positive  
435 correlation between GEM and TotHg thus implies that meteorological factors comprise the  
436 dominating process controlling mercury sources. Mercury emissions might - for instance - be  
437 influenced by changing sea surface temperatures or by large scale droughts leading to increased  
438 biomass burning (Monks et al., 2012). These examples are consistent with the observed GEM vs.  
439 SOI correlation.

440

441

## 442 **Acknowledgements**

443

444 The GEM measurements made at Cape Point have been supported by the South African Weather  
445 Service and have also received financial support from the Global Mercury Observing System  
446 (GMOS), a European Community funded FP7 project (ENV.2010.4.1.3-2). Furthermore, the  
447 collection and analysis of the precipitation samples have been financially supported by the  
448 Council for Scientific and Industrial Research (CSIR) and the National Research Foundation  
449 (NRF) of South Africa. We are also grateful to NOAA for their trajectory Hysplit model. We  
450 would also like to thank Robert Mason and Susan Gichuki from the University of Connecticut  
451 (USA) for their assistance with the rain sampler provision and set-up. We are grateful to Danie  
452 van der Spuy for the general maintenance of the Tekran analyser at Cape Point.

453

454

## 455 **References**

456

457 Biester, H., Kilian, R., Franzen, C., Woda, C., Mangini, A., Scholer, H.F. 2002 Elevated  
458 mercury accumulation in a peat bog of the Magellanic Moorlands, Chile (53°S) - an  
459 anthropogenic signal from the Southern Hemisphere. *Earth and Planetary Science Letters* 201,  
460 609-620.

461

462 Brunke, E.-G., Labuschagne, C., Parker, B., Scheel, H.E., Whittlestone, S. 2004. Baseline air  
463 mass selection at Cape Point, South Africa: Application of  $^{222}\text{Rn}$  and other filter criteria to CO<sub>2</sub>.  
464 *Atmospheric Environment* 38, 5693-5702.

465

466 Brunke, E-G., Labuschagne, C., Ebinghaus, R., Kock, H. and Slemr, F. 2010. Gaseous elemental  
467 mercury depletion events observed at Cape Point during 2007-2008. *Atmospheric Chemistry and*  
468 *Physics* 10, 1121-1131.



469  
470 Brunke, E.-G., Ebinghaus, R., Kock, H.H., Labuschagne, C., Slemr, F. 2012. Emissions of  
471 mercury in southern Africa derived from long-term observations at Cape Point, South Africa.  
472 *Atmospheric Chemistry and Physics* 12, 7465-7474.  
473  
474 Caffrey, J.M., Landing, W.M., Nolek, S.D., Gosnell, K.J., Bagui, S.S., Bagui, S.C. 2010.  
475 Atmospheric deposition of mercury and major ions to the Pensacola (Florida) watershed: spatial,  
476 seasonal, and inter-annual variability. *Atmospheric Chemistry and Physics* 10, 5425–5434.  
477  
478 Cole, A.S., Steffen, A., Eckley, C.S., Narayan, J., Pilote, M., Tordon, R., Graydon, J.A., Louis,  
479 V.L.St., Xu, X., Branfireun, B.A. 2014. A survey of mercury in air and precipitation across  
480 Canada: Patterns and trends. *Atmosphere* 5, 635-668.  
481  
482 Dabrowski, J.M., Ashton, P.J., Murray, K., Leaner, J.J., Mason, R.P. 2008. Anthropogenic  
483 mercury emissions in South Africa: Coal combustion in power plants. *Atmospheric Environment*  
484 42, 6620–6626.  
485  
486 Dutt, U., Nelson, P.F., Morrison, A.L., Strezov, V. 2009. Mercury wet deposition and coal-fired  
487 power station contributions: An Australian study. *Fuel Processing Technology* 90, 1354–1359.  
488  
489 Fitzgerald, W.F., Engstrom, D.R., Mason, R.P., Nater, E.A. 1998. The case for atmospheric  
490 mercury contamination in remote areas. *Environmental Science & Technology* 32, 1–7.  
491  
492 Gichuki, S.W., Mason, R.P. 2013. Mercury and metals in South African precipitation.  
493 *Atmospheric Environment* 79, 286-298.  
494  
495 Gratz, L. E., Keeler, G.J., Miller, E.K. 2009. Long-term relationships between mercury wet  
496 deposition and meteorology. *Atmospheric Environment* 43, 6218–6229.  
497  
498 Holmes, C.D., Jacob, D.J., Corbitt, E.S., Mao, J., Yang, X., Talbot, R., Slemr, F. 2010. Global  
499 atmospheric model for mercury including oxidation by bromine atoms. *Atmospheric Chemistry*  
500 *and Physics* 10, 12037-12057.  
501  
502 Kotnik, J., Horvat, M., Jereb, V. 2002. Modelling of mercury geochemical cycle in Lake  
503 Velenje, Slovenia. *Environmental Modelling & Software* 17, 593–611.  
504  
505 Lamborg, C.H., Rolfhus, K.R., Fitzgerald, W.F., Kim, G. 1999. The atmospheric cycling and air-  
506 sea exchange of mercury species in the South and equatorial Atlantic Ocean. *Deep-Sea Research*  
507 *II* 46, 957-977.  
508  
509 Laurier, F., Mason, R. 2007. Mercury concentration and speciation in the coastal and open ocean  
510 boundary layer. *Journal of Geophysical Research* 112, D06302, doi:10.1029/2006JD007320.  
511  
512 Lindberg, S., Bullock, R., Ebinghaus, R., Engstrom, D., Feng, X., Fitzgerald, W., Pirrone, N.,  
513 Prestbo, E., Seigneur, C. 2007. A synthesis in progress and uncertainties in attribution of sources  
514 of mercury in deposition. *Ambio* 36(1), 19-32.  
515  
516 Lombard, M.A.S., Bryce, J.G., Mao, H. Talbot, R. 2011. Mercury deposition in Southern New  
517 Hampshire, 2006–2009. *Atmospheric Chemistry and Physics* 11, 7657–7668.  
518



519 Masekoameng, K.E., Leaner, J., Dabrowski, J. 2010. Trends in anthropogenic mercury  
520 emissions estimated for South Africa during 2000 – 2006. *Atmospheric Environment* 44, 3007-  
521 3014.  
522

523 Mason, R.P., Sullivan, K.A. 1998. Mercury and methyl mercury transport through an urban  
524 watershed. *Water Research* 32, 321–330.  
525

526 Mason, R.P., Laporte, J.M, Andres, S. 2000. Factors controlling the bioaccumulation of  
527 mercury, methylmercury, arsenic, selenium and cadmium by freshwater invertebrates and fish.  
528 *Archives of Environmental Contamination and Toxicology* 38, 283 – 297.  
529

530 Mirlean, N., Larned, S.T., Nikora, V., Kutter, V.T. 2005. Mercury in lakes and lake fishes on a  
531 conservation-industry gradient in Brazil. *Chemosphere* 60, 226–236.  
532

533 Monks, S.A., Arnold, S.R., Chipperfield, M.P. 2012. Evidence for El Niño–Southern Oscillation  
534 (ENSO) influence on Arctic CO interannual variability through biomass burning emissions.  
535 *Geophysical Research Letters* 39, L14804, doi:10.1029/2012GL052512.  
536

537 Pirrone, N., Mason, R. 2009. *Mercury Fate and Transport in the Global Atmosphere: Emissions,  
538 Measurements and Models*, Springer, New York USA, 2009.  
539

540 Prestbo, E.M., Gay, D.A. 2009. Wet deposition of mercury in the U.S. and Canada, 1996–2005:  
541 Results and analysis of the NADP mercury deposition network (MDN). *Atmospheric  
542 Environment* 43, 4223–4233.  
543

544 Preston-Whyte, R.A., Tyson, P.D. 1988. *The Atmosphere and Weather of Southern Africa*.  
545 University of the Witwatersrand, Johannesburg, Oxford University Press, Cape Town, 375 pp.  
546

547 Rautenbach, C. J. de W., Smith, I.N. 2001. Teleconnections between global sea-surface  
548 temperatures and the interannual variability of observed and model simulated rainfall over  
549 southern Africa. *Journal of Hydrology* 254, 1-15.  
550

551 Scheel, H.E., Brunke, E-G., Sladkovic, R., Seiler, W. 1998. In situ CO concentrations at the sites  
552 Zugspitze (47 °N, 11 °E) and Cape Point (34 °S, 18 °E) in April and October 1994. *Journal of  
553 Geophysical Research* 103, D15, 19295-19304.  
554

555 Schroeder, W. H., Munthe, J. 1998. Atmospheric mercury - an overview. *Atmospheric  
556 Environment* 32, 809-822.  
557

558 Seiler, W., Giehl, H., Halliday, E.C., Brunke E-G. 1984. The seasonality of carbon monoxide  
559 abundance in the Southern Hemisphere. *Tellus* 36B, 4, 219-231.  
560

561 Slemr, F., Brunke, E.-G., Labuschagne, C., Ebinghaus, R. 2008. Total gaseous mercury  
562 concentrations at the Cape Point GAW station and their seasonality, *Geophys. Res. Lett.*, 35,  
563 L11807, doi:10.1029/2008GL033741.  
564

565 Slemr, F., Brunke, E.-G., Ebinghaus, R., Kuss, J. 2011. Worldwide trend of atmospheric  
566 mercury since 1995. *Atmospheric Chemistry and Physics* 11, 4779-4787.  
567

568 Slemr, F., Brunke, E.-G., Whittelstone, S., Zahorowski, W., Ebinghaus, R., Kock, H.H.,  
569 Labuschagne, C. 2013. <sup>222</sup>Rn-calibrated mercury fluxes from terrestrial surface of southern  
570 Africa. *Atmospheric Chemistry and Physics* 13, 6421-6428.  
571

572 Soerensen, A.L., Jacob, D.J., Streets, D.G., Witt, M.L.I., Ebinghaus, R., Mason, R.P.,  
573 Andersson, M., Sunderland, E.M. 2012. Multi-decadal decline of mercury in the North Atlantic  
574 atmosphere explained by changing subsurface seawater concentrations. *Geophysical Research*  
575 *Letters* 39, L21810, doi:10.1029/2012GL053736.  
576

577 Sprovieri, F., Pirrone, N., Ebinghaus, R., Kock, H., Dommergue, A. 2010. A review of  
578 worldwide atmospheric mercury measurements. *Atmospheric Chemistry and Physics* 10, 8245-  
579 8265.  
580

581 Steffen, A., Schroeder, W. 1999. Standard operation procedures manual for total gaseous  
582 mercury measurements, Canadian Mercury Measurement Network (CAMNet), Version 4.0.  
583

584 Streets, D.G., Devane, M.K., Lu, Z., Bond, T.C., Sunderland, E.M., Jacob, D.J. 2011. All-time  
585 releases of mercury to the atmosphere from human activities. *Environmental Science &*  
586 *Technology* 45, 10485-10491.  
587

588 US EPA (United States Environmental Protection Agency). 1996. Method 1669: sampling  
589 ambient water for trace metals at EPA water quality criteria levels. EPA publication no.: 821-R-  
590 96-008. Washington DC, USA.  
591

592 Williams, C.R., Leaner, J.J., Nel, J.M., Somerset, V.S. 2010. Mercury concentrations in water  
593 resources potentially impacted by coal-fired power stations and artisanal gold mining in  
594 Mpumalanga, South Africa. *Journal of Environmental Science & Health A45*, 1363–1373.  
595

596 Williams, C.R., Leaner, J.J., Somerset, V.S., Nel, J.M. 2011. Mercury concentrations at a  
597 historically mercury-contaminated site in KwaZulu-Natal (South Africa). *Environmental Science*  
598 *and Pollution Research* 18, 1079–1089.  
599

600 Wilson, S., Munthe, J., Sundseth, K., Kindbom, K., Maxson, P., Pacyna, J., Steenhuisen, F.  
601 2010. Updating historical global inventories of anthropogenic mercury emissions to air. AMAP  
602 Tech. Rep. 3, 14 pp., Arctic Monitoring and Assessment Programme, Oslo.  
603

604 Xu, L.Q., Liu, R.H., Wang, J.Y., Tan, A.K., Yu, P. 2012. Mercury emission flux in the Jiaozhou  
605 Bay measured by flux chamber. *Procedia Environmental Sciences* 13, 1500-1506.  
606  
607

## Mercury measurements (2007-2013) made in the atmosphere and in rainwater at Cape Point, South Africa

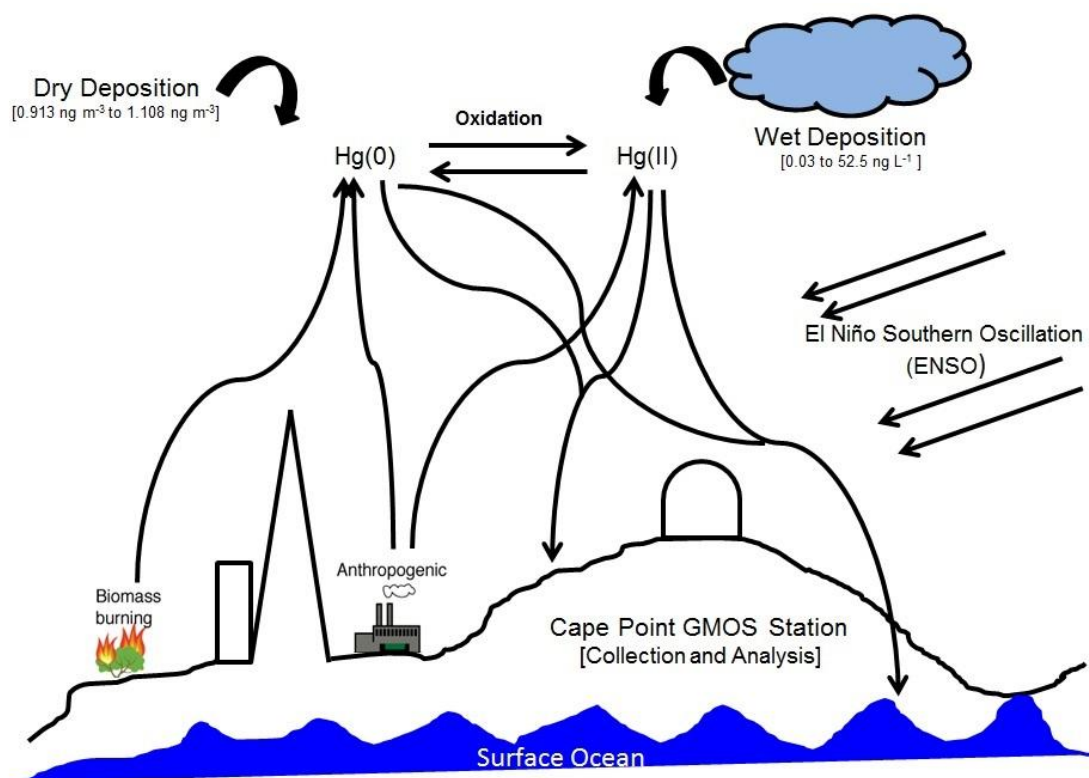
Ernst-Günther Brunke<sup>1</sup>, Chavon Walters<sup>2</sup>, Thumeka Mkololo<sup>1</sup>, Lynwill Martin<sup>1</sup>, Casper Labuschagne<sup>1</sup>, Bongwiwe Silwana<sup>2</sup>, Franz Slemr<sup>3</sup>, Andreas Weigelt<sup>4</sup>, Ralf Ebinghaus<sup>4</sup>, and Vernon Somerset<sup>2‡</sup>

<sup>1</sup>South African Weather Service c/o CSIR, P.O. Box 320, Stellenbosch 7599, South Africa

<sup>2</sup>Natural Resources and the Environment (NRE), Council for Scientific and Industrial Research (CSIR), Stellenbosch, 7600, South Africa.

<sup>3</sup>Max-Planck-Institut für Chemie, Hahn-Meitner-Weg 1, 55128 Mainz, Germany

<sup>4</sup>Helmholtz-Zentrum Geesthacht (HZG), Institute of Coastal Research, Max-Planck-Strasse 1, D-21502 Geesthacht, Germany,



‡ Vernon Somerset; Tel.: +27.21.8882631; Fax: +27.86.6631789; Email: [vsomerset@csir.co.za](mailto:vsomerset@csir.co.za); [vsomerset@gmail.com](mailto:vsomerset@gmail.com)

## Mercury measurements (2007-2013) made in the atmosphere and in rainwater at Cape Point, South Africa

Ernst-Günther Brunke<sup>1</sup>, Chavon Walters<sup>2</sup>, Thumeka Mkololo<sup>1</sup>, Lynwill Martin<sup>1</sup>, Casper Labuschagne<sup>1</sup>, Bongwiwe Silwana<sup>2</sup>, Franz Slemr<sup>3</sup>, Andreas Weigelt<sup>4</sup>, Ralf Ebinghaus<sup>4</sup>, and Vernon Somerset<sup>2‡</sup>

<sup>1</sup>South African Weather Service c/o CSIR, P.O. Box 320, Stellenbosch 7599, South Africa

<sup>2</sup>Natural Resources and the Environment (NRE), Council for Scientific and Industrial Research (CSIR), Stellenbosch, 7600, South Africa.

<sup>3</sup>Max-Planck-Institut für Chemie, Hahn-Meitner-Weg 1, 55128 Mainz, Germany

<sup>4</sup>Helmholtz-Zentrum Geesthacht (HZG), Institute of Coastal Research, Max-Planck-Strasse 1, D-21502 Geesthacht, Germany,

### Highlights

- Extended summary provided of GEM and THg measured at Cape Point, South Africa.
- Positive correlation observed between GEM and TotHg concentrations.
- Meteorological factors such as the El Niño Southern Oscillation (ENSO) contributed.
- Mercury emissions are influenced by increased biomass burning in drier seasons.
- Data presented provides novel information on atmospheric behaviour of mercury.

---

<sup>‡</sup> Vernon Somerset; Tel.: +27.21.8882631; Fax: +27.86.6631789; Email: [vsomerset@csir.co.za](mailto:vsomerset@csir.co.za); [vsomerset@gmail.com](mailto:vsomerset@gmail.com)